Analysis of Detection Performance of Incoherent Range Walk Compensation for Passive Radar

Erlend Finden*, Jonas Myhre Christiansen*, Øystein Lie-Svendsen* and Karl Erik Olsen*

*Norwegian Defence Research Establishment
P.O.Box 25, NO-2027 Kjeller, NORWAY
email: erlend.finden@ffi.no

Abstract: *This paper analyzes the performance of an incoherent range walk compensation method for passive radar systems. The method utilizes the velocity information in the range-Doppler map, and no detection before compensation is demanded. Our contribution is to analyze the performance on data from actual measurements of Digital Video Broadcast-Terrestrial (DVB-T) signals in the UHF band. Detection thresholds for a specified false alarm probability were computed from an Erlangian probability distribution, with moments estimated from the data. Two different targets in two datasets were studied. Extending the integration time from 0.26 s and 0.52 s to 4.2 s caused an increase in the target to threshold ratio of 5-7 dB. The method is limited to targets with little Doppler walk during the integration time. Final conclusions on detection performance cannot be made until more targets have been analyzed.*

1. Introduction

In recent years effort has been spent on improving the performance of passive radars [1]. If higher processing gain is desired, it is crucial to increase the integration time. However, long integration time may cause detection problems for maneuvering targets [1], [2]. One issue arises when illuminators of opportunity of high-bandwidth waveforms are exploited. Since high bandwidth yields fine range resolution, a decorrelation in the range dimension (range walk), is likely to be observed during the integration time for targets of high bistatic velocity. Extending the coherent integration time also leads to finer velocity resolution. Thus targets of non-zero bistatic acceleration are also likely to experience Doppler walk, which spreads energy in the Doppler dimension. Methods to coherently compensate range walk for targets of constant bistatic velocity in passive radar have been presented e.g. [3], [4]. Other works additionally compensate Doppler walk as in [5], [1], [6]. The expected advantage of coherent methods is high integration gain. Nevertheless, depending on the application of the methods, other properties, such as computational burden and the necessity of detection before compensation (as is the case in [6]), should be considered. Not much work has been presented on incoherent compensation of range walk for passive radar, except for the method introduced by [7]. The method does not require much processing power, and does not demand detection before compensation, since all targets at all Doppler frequencies are compensated. However, the method will be successful only for targets of constant bistatic velocity. Our contribution is to analyze the detection performance of this method, extending the results presented in [7].

Dette er en postprint-versjon / This is a postprint version.
DOI til publisert versjon / DOI to published version: 10.1109/IRS.2015.7226261

2. Range Walk Compensation

A passive radar built by Fraunhofer FHR in Germany was applied for recording two datasets, containing Norwegian Digital Video Broadcast-Terrestrial (DVB-T) transmissions. DVB-T channels of different carrier frequencies were selected for the two datasets, 722 MHz and 538 MHz, both of 8 MHz bandwidth. A reference antenna and a surveillance antenna were used to sample reference and surveillance channels r and s, respectively. After down-conversion and decimation, the simplified cross-correlation function presented in e.g. [8], [9] was applied:

$$\chi_p(l,m) = \sum_{j=0}^{A-1} \sum_{k=0}^{N-1} s(Sp+k+jN+l) r^*(Sp+k+jN) e^{-i\frac{2\pi jm}{A}} \tag{1}$$

Here $A, N > 0$ are integers satisfying $S = AN$ where S is the number of samples in the coherent integration interval t_c. l is the time delay index, and m is the Doppler index related to the Doppler frequency. The index p is a positive integer, introducing a delay in start time for the cross correlation function χ_p. The range walk compensation method presented by [7] utilizes the Doppler information available in the range-Doppler map (1). During coherent integration of M successive intervals, enumerated p, each of duration t_c, targets that do not change bistatic velocity v will migrate a distance pt_cv during the integration time pt_c. The displacement is compensated in each Doppler column for each of the M cross-correlation functions, before being summed incoherently,

$$\hat{\chi}(l,m) = \sum_{p=0}^{M-1} |\chi_p(l - \lfloor \frac{mf_sp}{f_c} \rfloor, m)|^2 \tag{2}$$

Here f_s and f_c are the sampling and carrier frequencies, respectively. The sum of squares in (2) is chosen in order to obtain a closed form of the noise distribution (a different form was used in [7]). For detection purposes, the advantage of the incoherent range walk compensation (IRWC) (2) is that the Doppler resolution is given by the inverse of the coherent integration time, t_c^{-1}, only. Hence targets that are distributed over a constant Doppler region during the incoherent integration time $T_I = Mt_c$, will not be dispersed into several Doppler cells. Targets are expected to achieve optimum performance in the IRWC-method when integrated coherently over as long a period as possible without experiencing range walk. This is achieved when applying the coherent integration time t_c, which allows for targets to migrate approximately one bistatic range cell ΔR, i.e.

$$t_c \sim \frac{\Delta R}{|v|} \tag{3}$$

Applying the chosen t_c in the compensation of a target of significantly different bistatic velocity from that intended, are expected to yield a non-optimal result in the compensation, as pointed out by [11]. If high detection performance of targets in the entire Doppler region is desired, it is suggested to calculate different versions of (2) of various values of t_c in parallel [11]. The number of parallel computations can be limited, as targets of somewhat different bistatic velocity may be integrated with a common t_c. E.g. targets with $v = 140-180$ m/s, travel $36-47$ m in $t_c = 0.26$ s, which is not much more than one bistatic range cell (37.5 m).

Dette er en postprint-versjon / This is a postprint version.
DOI til publisert versjon / DOI to published version: 10.1109/IRS.2015.7226261

3. Signal to Noise Ratio

We obtain the noise distribution from the range-Doppler bins given by

$$U_p = \chi_p^2(l,m),\ l = \{a,..,b\} \text{ and } m = \{m' - c,..,m' + c\} \tag{4}$$

Here the subscript index p denotes the starting time interval of the cross-correlation function, m' is the center Doppler bin in the region to extract the noise. a, b and c are positive integers, defining the boundary of the noise sample. Due to variations in the noise level with range and Doppler, different noise samples are chosen for different sections of the range-Doppler map. If present, known peaks in the cross-correlation function caused by the DVB-T signal and the zero-Doppler line are removed from the noise sample. Potential targets are, however, included in the noise sample. Likewise, the noise in the incoherent integration (2) is here defined as the set of bins

$$\hat{U} = \hat{\chi}(l,m),\ l = \{a,..,b\} \text{ and } m = \{m' - c,..,m' + c\} \tag{5}$$

For the two datasets, $\sim 4 \cdot 10^4$ bins represented the noise in U_p and $\hat{U}$. The signal to noise ratio (SNR) for the coherent integration is here defined as

$$SNR(l,m) = 10 \log 10 \frac{\chi_p^2(l,m)}{< U_p >} \tag{6}$$

where the mean of U_p is denoted as $< U_p >$. The two datasets (Dataset 1 and Dataset 2) each contained a target (Target 1 and Target 2). Target 1 and Target 2 had a bistatic velocity of -141 m/s and -118 m/s, respectively, remaining approximately constant over the first 6 s. The peak value of the SNR for the two targets are presented as a function of t_c in Table 1. For both targets, after ~ 0.5 s range walk causes the SNR to decrease.

t_c (s)	0.13	0.26	0.52	1.1	2.1	4.2
Peak SNR Target 1 (dB)	13.6	18.7	18.3	13.2	12.7	12.8
Peak SNR Target 2 (dB)	19.9	22.8	21.1	18.2	14.6	15.7

Table 1: The peak value of the target SNR (6) for each coherent integration time, t_c.

4. Threshold Detection

As indicated in [10], the DVB-T baseband signal excluding pilots and guard interval is expected to be a white Gaussian process. Hence, the noise samples U_p can be approximated by an exponential probability density function (pdf) $\rho(x)$:

$$\rho(x) = \beta_p e^{-\beta_p x} \tag{7}$$

where

$$\beta_p^{-1} =< U_p > \tag{8}$$

Dette er en postprint-versjon / This is a postprint version.
DOI til publisert versjon / DOI to published version: 10.1109/IRS.2015.7226261

Modeling the coherent noise samples U_p as random independent variables that follow an exponential distribution, it follows that $\hat{U}$ is a sum of exponentially distributed variables. If the different U_p, which constitute the noise in each of the M terms in the sum (2), all yield the same β_p, $\beta_p = \beta$, $\hat{U}$ can be modeled as the Special Erlangian probability distribution [12]

$$\rho(x) = \frac{\beta^M x^{M-1} e^{-\beta x}}{\Gamma(M)} \tag{9}$$

For the IRWC-method the detection enhancement can be described as follows. As the incoherent integration time is increased by increasing M, a possible target signal and the noise level will both increase equally in magnitude. Hence there is no increase in SNR. However, the relative fluctuation in the noise $\hat{U}$ decreases. Thus, for a specified false alarm probability P_{FA}, the ratio between a target signal and the detection threshold increases. The detection threshold x_T is calculated from

$$\int_{x_T}^{\infty} \rho(x) dx = P_{FA} \tag{10}$$

Substituting (9) in (10) and integrating by parts yields

$$P_{FA} e^{\beta x_T} = \sum_{j=1}^{M} \frac{(\beta x_T)^{M-j}}{(M-j)!} \tag{11}$$

The transcendental equation (11) can be solved numerically with respect to x_T. Let us define the ratio between a target located at $l = l'$ and $m = m'$ and the threshold for the IRWC-method as

$$\Delta_I = 10 \log 10 \frac{\hat{\chi}(l', m')}{x_T} \tag{12}$$

We find that the observed variations in β_p are so small that they have negligible influence on the computation of Δ_I (of order 0.5 dB), so that treating β_p as constant is a valid approximation for our datasets. Moreover, histograms of the noise $\hat{U}$ show good agreement with the modeled Erlangian pdf, and hence the calculation of thresholds with the analytical expression (11) is justified. This is shown for Dataset 2 in Fig 1, where also thresholds for $P_{FA} = 10^{-6}$ are included.

5. Results

Applying the IRWC-method to the two datasets and calculating detection thresholds for $P_{FA} = 10^{-6}$ yields the target to threshold ratios for the two targets shown in Fig. 2. Target 1 shows best performance in target to threshold ratio for $t_c = 0.26$ s, while a corresponding increase for Target 2 is observed when $t_c = 0.52$ s. To some extent, this reflects the criteria in (3), which yields $t_c \sim 0.27$ s for Target 1 and $t_c \sim 0.32$ s for Target 2. For both targets, the target signal and the noise both increase equally in magnitude up to $T_I = 4.2$ s (not shown). However, the target to threshold ratio is observed to increase more rapidly at low M values. Furthermore, extending the integration time from 4.2-8.4 s yields no increase in target to threshold ratio due to a decrease in the peak target signals (not shown). While the target in Dataset 1 lost signal

Dette er en postprint-versjon / This is a postprint version.
DOI til publisert versjon / DOI to published version: 10.1109/IRS.2015.7226261

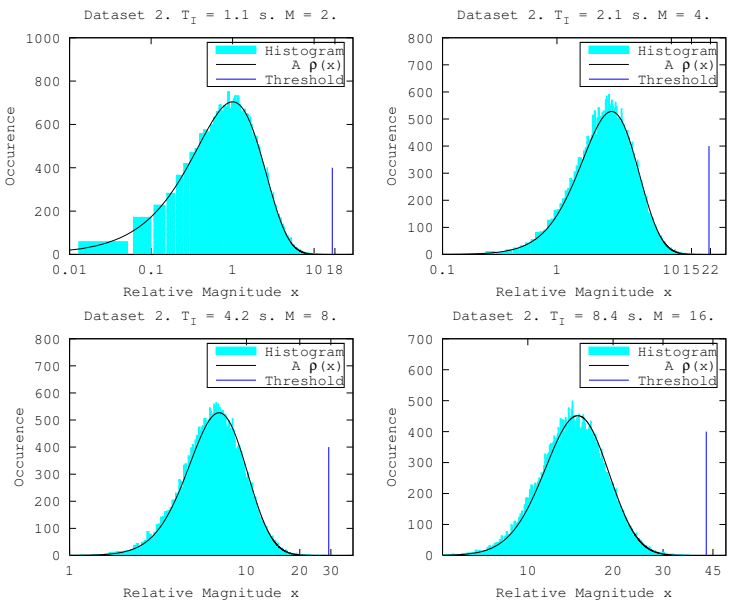

Figure 1: Histograms of the noise in Dataset 2 from the IRWC-method (5), plots of $\rho(x)$ from (9) multiplied by the area A under the histogram and detection thresholds for $P_{FA} = 10^{-6}$. The noise are presented in relative magnitude as $x = \frac{\hat{U}}{<U_1>}$. $t_c = 0.26$ s.

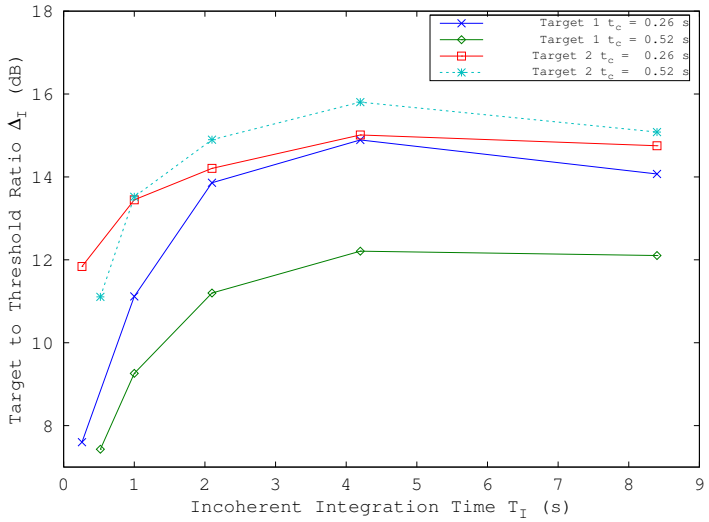

Figure 2: Target to threshold ratio Δ_I with the IRWC-method as a function of incoherent integration time T_I, for Target 1 and Target 2. $P_{FA} = 10^{-6}$.

strength after 6 s when integrated with $t_c = 0.26$ s, the decrease in peak target signal in Dataset 2 is probably due to Doppler walk, which is present after ~ 6 s. Increasing the integration time for Target 1 from 0.26-4.2 s yields a total increase in target to threshold ratio of nearly 7 dB. In contrast, coherent integration is in theory expected to yield, if the range walk compensation is performed perfectly, 12 dB gain [13]. For Target 2, increasing the integration time from 0.52-4.2 s, yields a total increase in the target to threshold ratio of nearly 5 dB.

Dette er en postprint-versjon / This is a postprint version.
DOI til publisert versjon / DOI to published version: 10.1109/IRS.2015.7226261

6. Conclusion

For the two datasets studied here, the IRWC-method was found to give an increase of 5-7 dB in target to threshold ratio when the integration time was extended from 0.26 s and 0.52 s to 4.2 s, respectively. This result is within the expected enhancement range for incoherent integration, which is between a 1.5 dB and 3 dB for each doubling of the integration time [13]. For both targets, from 4.2 s to 8.4 s the method gave no further enhancement, due to loss of target signal and Doppler walk, the latter being the limiting factor of the IRWC-method. Before final conclusions on the performance can be drawn, the method has to be applied to more than the two targets analyzed here.

References

[1] M. Malanowski, "Detection and parameter estimation of manoeuvring targets with passive bistatic radar", *IET Radar, Sonar & Navigation*, 2012, vol. 6, no.8, pp. 739-745.

[2] M. Malanowski and K. Kulpa, "Analysis of integration gain in passive radar", in *Proc. 2008 IEEE Int. Conf. Radar*, Adelaide, Australia, September 2008, pp. 323-328.

[3] K. Kulpa and J. Misiurewicz, "Stretch processing for long integration time passive covert radar", in *Proc. 2006 CIE Int. Conf. Radar*, Shanghai, China, October 2006, pp. 1-4.

[4] W. C. Barott and J. Engle, "Single-antenna ATSC passive radar observations with remodulation and keystone formatting", in *Proc. 2014 IEEE Radar Conf.*, Cincinnati, USA, May 2014, pp. 159-163.

[5] M. Malanowski, et al., "Extending the integration time in DVB-T-based passive radar", in *Proc. 2011 European Radar Conf. (EuRAD)*, Manchester, United Kingdom, October 2011, pp. 190-193.

[6] J. M. Christiansen et al., "Coherent range and Doppler-walk compensation in PBR applications", in *Proc. 2014 Int. Radar Symp. (IRS)*, Gdansk, Poland, June 2014, pp. 32-36.

[7] J. M. Christiansen and K. E. Olsen, "Range and Doppler walk in DVB-T based passive bistatic radar", in *Proc. 2010 IEEE Radar Conf.*, Arlington, USA, May 2010, pp. 620-626.

[8] D. Langellotti et al., "Comparative study of ambiguity function evaluation algorithms for passive radar", in *Proc. 2009 Int. Radar Symp. (IRS)*, Hamburg, Germany, September 2009, pp. 325-329.

[9] P. Lombardo and F. Colone, "Advanced Processing Methods for Passive Bistatic Radar Systems", in *Principles of Modern Radar: Advanced Techniques*, W. L. Melvin and J. A. Scheer, Eds. Edison, NJ: SciTech Publishing, 2013, pp. 751.

[10] M. Cherniakov, "Ambiguity Function Correlation in Passive Radar: DTV-T Signal", in *Bistatic Radar - Emerging Technology*, M. Cherniakov, Ed. Chichester, England: John Wiley & Sons Ltd. 2008, pp. 317-318.

[11] J. M. Christiansen, "DVB-T based Passive Bistatic Radar", M.S. thesis, Dept. of Eng. Cybern., Norwegian University of Science and Technology, Trondheim, Norway, 2009.

[12] E. Lloyd, "A Catalogue of Continuous Probability Distributions", in *Handbook of Applicable Mathematics - Volume II: Probability*, W. Ledermann, Ed. New York: John Wiley & Sons Ltd, 1980, pp. 202.

[13] M. A. Richards, "Digital Signal Processing Fundamentals for Radar", in *Principles of Modern Radar - Basic Principles*, M. A. Richards et al., Eds. Raleigh, NC: SciTech Publishing, 2010, pp. 536-538.

DOI til publisert versjon / DOI to published version: 10.1109/IRS.2015.7226261